

Life Prediction and Determination for Austenitic Stainless Steel

Hassan Osman^{1,2}, Mohyeldin Ahmed¹, M.N. Tamin², Mohamed H. M. Faris¹

¹Mechanical Engineering Department, Sudan University of Science and Technology, Khartoum, Sudan 11111

²Faculty of Mechanical Engineering-Universiti Teknologi Malaysia

E-mail: hassaninsan @ gmail.com; mohamedhfaris @ gmail.com

Abstract— The development of improved efficiency microturbine necessitates the evaluation of stainless steel foil for elevated temperature applications as the primary surface, plate and fins in the recuperator system. This study is aimed at extending the operating temperature limit of Type 347 austenitic stainless steel foils. Foil forms of the stainless steel alloy 347 have been examined in an 'as processed' condition and following creep-rupture testing in air at 650-750 °C and 54-221MPa. Prior to creep testing, the microstructure consists of γ phase with NbC precipitates. Experimental data of creep test for thin foil shows different nature from the bulks material. In a time 104 s (about 3 hours) the foils specimen deform elastically with some specimen tested under higher stress level deformed with power law creep mechanism, and of order 10-4 to 10-3. At low level of applied stress the strain for the foil reached already the order of 10% with diffusional flow domination mechanism and at higher stress level Power law mechanism is dominated. Creep data will be based on accelerated tests where the stresses or temperature are higher. A very fundamental issue is then how to extrapolate the accelerated test data to the operational conditions. In this respect a various methods is discussed such as Larson-Miller plots, Orr-Sherby-Dorn, and Manson-Succop.

Keywords— Austenitic stainless steel foil, failure-mechanism, creep rate, Iso-stress.

I. INTRODUCTION

An increase in efficiency of microturbines (100 kW_e) to 40 percent is possible with the increase of turbine inlet temperature to 1230 degree Celsius [1, 2]. Consequently, the heat exchanger or recuperator system is required to operate at inlet temperature up to 843 degree Celsius. Current primary surface recuperators utilize AISI 347 stainless steel foils and operate at limiting temperature of 650 degree Celsius. Limited published test data on the long-term deformation response of AISI 347 stainless steel foils at elevated temperature is available [1, 3]. While properties and behavior of AISI 347 steel is generally known for processing and fabrication into other high-temperature components such as heat-exchanger piping and gas turbine parts, information on these alloys fabricated into thin foils (0.1–0.25 mm-thick) for use in primary surface recuperators is limited or nonexistent. This study is addressing creep behavior and life prediction of AISI 347 steel foils at high homologous temperature. Limited creep tests on commercial AISI 347 steel recuperator stock has been conducted [3]. Aging effects on the steel up to 30,000 hours at temperatures above 700 degree Celsius have been established in terms of detrimental sigma phase formation [4]. Several stainless alloys including modified alloy 803 (25Cr, 35Ni),

alloy 230 (22Cr, 52.7Ni, 2Mo) and alloy 120 (25Cr, 32.3Ni, 0.7Nb, 2.5Mo) [5] showed better creep strength at 750 degree Celsius than AISI 347 stainless steel but at noticeable increase in materials cost. Although Ni-based superalloys such as Inconel 625(Ni-21Cr) have sufficient oxidation and creep resistance for use up to 700 °C, the cost is, however, 3.5-4 times that of steel [6].

The overall objective of this study is to quantify the creep responses, deformation mechanisms and prediction of long-term creep response of AISI 347 stainless steel foils at isothermal test temperature (650 - 700 degree Celsius) and applied stress up to 221 MPa as part of accelerated test program. The test data establishes baseline information for extending the operating temperature limit of the steel foils while maintaining cost competitiveness of recuperator materials. Emphasis is placed on creep parameters of the steel foils including the minimum creep rate, creep strain at rupture and rupture time. Rupture time is an important design parameter for recuperator foils operating in the high-temperature creep regime over long service life. Prediction of long-term creep response from short-term creep-rupture test data of metals is possible using Larson-Miller parameter [7] and Orr-Sherby-Dorn parameter [8] that relates the applied stress to temperature and rupture life.

II. LITERATURE REVIEW

Both Larson-Miller and Orr-Sherby-Dorn formulations express iso-stress creep data in terms of logarithmic time as a linear function of reciprocal temperature. The former assumes that all iso-stress lines converge at a common point on the (log(t)-1/T) plot while the latter plots parallel iso-stress lines. Larson-Miller parameters are obtained by assuming that activation energy is independent of applied stress. In Orr-Sherby-Dorn approach, the activation energy is assumed to remain constant over the entire creep curve, and be independent of temperature. Since plots of stress versus Larson-Miller or Orr-Sherby-Dorn parameter often exhibit a pronounced curvature, these relationships can only offer reliable extrapolation of failure times over a limited range of stress or temperature. At longer creep exposure times, effects of temperature- or irradiation-induced phase reactions or changes in creep mechanisms could not be accounted for in these phenomenological creep models based on accelerated range of creep data. Stefan Holmström et al. in their study for creep-fatigue behavior of 316 stainless steel established models for predicting creep strain and rupture of 316L, using

the Wilshire equations. [9]. Husam Al-Warmizyari et al investigated the degradation in creep strength for the austenitic stainless steel tube metal. The results were compared with data of non-serviced samples of the same metal type. The sample is tested for temperature within range (700-750 C) and stress (120-140 MPa). The results shows that the alloy exhibits a reduction in creep strength after long service life in comparisons with the non-serviced metal samples. The creep curves also reveal that the third stage of the serviced samples is the longest creep stages, while for the non-serviced samples the second stage is the longest. Also the microstructure of the serviced sample shows that creep voids start to nucleate on the grain boundaries at creep life around 60% of the creep rupture life [10].

III. MATERIALS AND EXPERIMENTAL PROCEDURES

The AISI 347 austenitic stainless steel foils used in this study is supplied in rolled and annealed condition. The foil thickness is 0.25 mm. The chemical composition of the foil is (in wt. %) 17.8Cr, 11.0Ni, 0.1Mo, 0.64Nb, 0.03C, 0.6Si, 1.6Mn, 0.04Ti, the balance being Fe. The high content of chromium and nickel results in adherent, stable chromium oxide or nickel oxide film for corrosion-resisting property of the material. The addition of 17.8Cr and 11Ni modified the Fe-C phase diagram such that the particularly stable phase austenite that formed at elevated temperature tends to be retained after annealing [11]. The low carbon content (0.03 wt. %) improves weldability and resistance to carbide precipitation. The addition of Nb further improves in suppressing carbide precipitation at grain boundaries. Figure 1 shows microstructure of the as-received foil that consists of austenite matrix with transformed carbide phase. Rolling effects is suppressed by annealing and only apparent in the elongated grains in the thickness cross-section of the foil.

Thin foil creep specimens are wire-cut from large sheet to the specimen geometry. Series of creep-rupture tests are performed at 650 - 700±2 degree Celsius, with applied stress levels ranging from 54 to 221 MPa in a dead-load creep testing machine with a 3-zone furnace. Effective gage length of the specimen is determined in accordance to ASTM E139 standards [12].

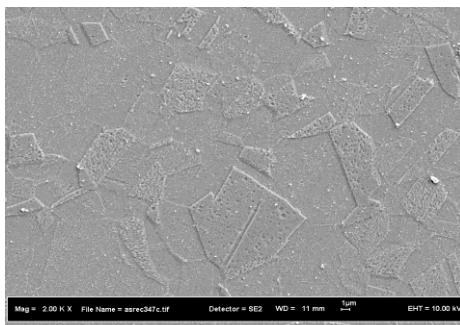


Fig. 1. Microstructure of as-received AISI 347 stainless steel foil.

IV. RESULTS AND DISCUSSION

A) Application of deformation maps to analyze creep test conditions for the foil

During plastic deformation of metals a number of deformation processes with different mechanisms may occur

simultaneously. However a single mechanism would favorably dominate the deformation. The predominating deformation mechanism is determined by the strain rate, applied stress, temperature and the grain size of the specimen. Ashby [13] proposed a mechanism map located in a field of two coordinates, temperature and stress to characterize the predominant deformation mechanism. Figure (2-4) shows the creep deformation maps for both the steady-state and transient flow of 316 stainless steel.

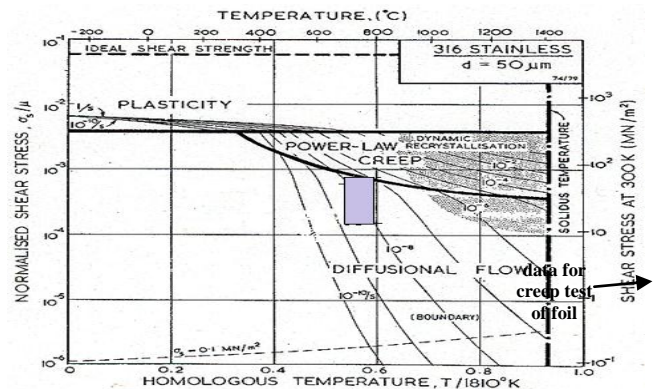


Fig. 2. A steady-state map for 316 stainless steel with a grain size of 50 μm, showing the operating conditions of the austenitic foil, and the dominant steady-state flow mechanisms.

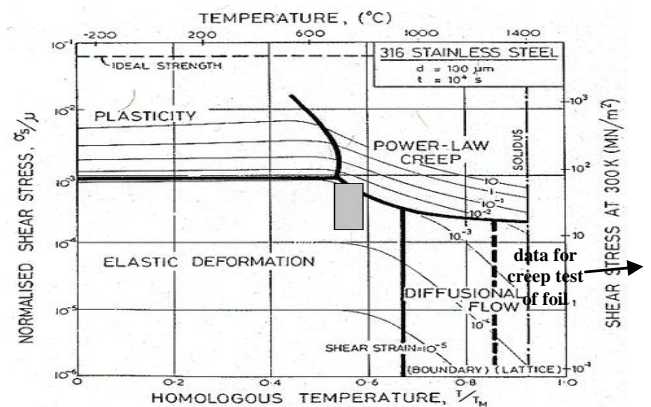


Fig. 3. A transient map for 316 stainless steel with a grain size of 100 μm, showing the strains which appear in 104 s (3 hours). All foils specimen deform elastically with some deformed under power law creep.

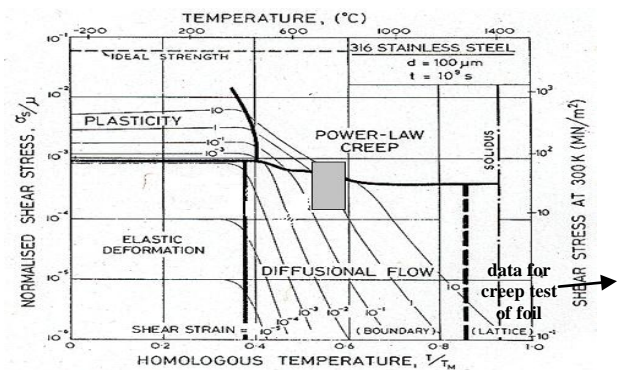


Fig. 4. A transient map showing the strains accumulated in 109 s (30 years). All foils specimen have suffered creep strain exceed 10%. Deformation is dominated by diffusional flow and power law creep.

Figure 3 and 4 is a transient maps for 316 stainless steel with a grain size of 100 μm showing the strain reached in a

given time, and the mechanism principally responsible for that strain. In a time 104 s (about 3 hours, Figure 3) the result shows that all the foils specimen deform elastically with some specimen tested under higher stress level deformed with power law creep mechanism, and of order 10-4 to 10-3. As time elapses, the creep strains grow, Figure 4 shows the creep rate after 109 s (30 years). Creep strain for the foil reached already the order of 10% at low level of applied stress with diffusional flow domination mechanism. Power low creep mechanism is dominant at higher stress level.

B) Prediction of rupture life on long term creep

Creep damage is a major life limiting factor for components operate at high temperatures. Thus, the correlation between rupture life and creep characteristics is the subject of the number of studies conducted in the past which suggested some methods for predicting creep life during long time at high temperature service.

The conventional method of evaluating creep behavior has been applied via stress versus time to rupture. The logarithm plot of stress versus rupture time is often found to be in linear form, which indicates that there is no change in principal mechanism [14]. The variation of rupture life with applied stress for 347 steel foil shown in Figure 5. The relationship between rupture life and applied stress was found to be in power law as $t_r = B\sigma^{-n}$ with stress exponent $n=3.3$.

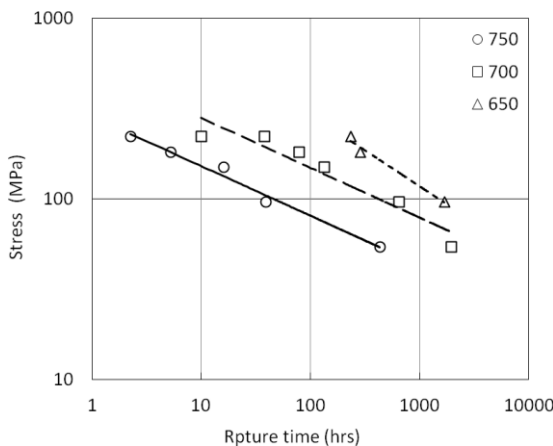


Fig. 5. Log-log applied stress versus rupture life for creep

The prediction of creep rupture life is evaluated using iso-stress lines base model. These models represent the rupture data by a parametric master curve. The plotting of a semi-log graph for creep rupture life t_r versus the temperature T will produce parallel iso-stress lines as shown in Figure 6, with slope B , this method is used to calculate Manson–Succop parameter in the form of the following equation [15]

$$P_{MS} = \log(t_r) - BT, \tag{1}$$

The Orr–Sherby–Dorn parameters also derived from the expression of secondary creep strain rate at a constant stress as [16]: The parameter for Orr-Sherby-Dorn life prediction method is also derived by considering the expression for the secondary creep strain rate at constant stress.

$$P_{OSD} = \log t_r - \frac{Q}{RT}, \tag{2}$$

where t_r is the time to rupture at temperature T , Q a characteristic activation energy for the process and R the universal gas constant. Similarly the Larson–Miller parameter is calculated with the assumption that activation energy is independent of applied stress [17]. This technique is reliable for life prediction as long the microstructure of the alloy is stable during it is exposure at high temperature [18, 19]:

$$P_{LM} = T(\log t_r + C). \tag{3}$$

The activation energy for creep, Q_c , can be defined for a constant stress condition as:

$$Q_c = \left. \frac{d \ln \dot{\epsilon}_m}{d \left(\frac{-1}{RT} \right)} \right|_{\sigma=const} \tag{4}$$

The resulting apparent activation energy for creep of AISI 347 steel foil at 96 MPa is 676.4 kJ.mol⁻¹. Luo Hai-Wen et al [20] found the activation energy for hot working AISI 347 stainless steel to be 520 - 590 kJ/mol. The higher value in Q_c indicates that AISI 347 stainless steel exhibits stronger creep resistance than other austenitic stainless steel during rolling at high temperature. This is presumably due to the high content of Nb at 0.7 % in the AISI 347 stainless steel. Since the foil specimen experienced greater resistance offered by the precipitates to the dislocation movement, a higher value of activation energy is justified

This value of creep activation energy was calculated based on minimum creep rates. However, over the full range of strain rates it is further postulated that diffusion in the foils could take place preferentially along dislocation when lattice diffusion is difficult. In such case, the activation energy should be taken as 0.5 Q_c [21] or 332 kJ/mol. This value is used in calculating the Orr–Sherby–Dorn parameters as shown in Figure 7a.

The different parameterization curves obtained in each case is shown in Figure 7. It can be noticed that the results are approximately equivalent. With slightly better fit for the Manson–succop analysis. Due to the limited amount of creep data obtained in the present work of relatively short durations it is difficult to attribute any reason why the Manson–Succop methods showed the better results.

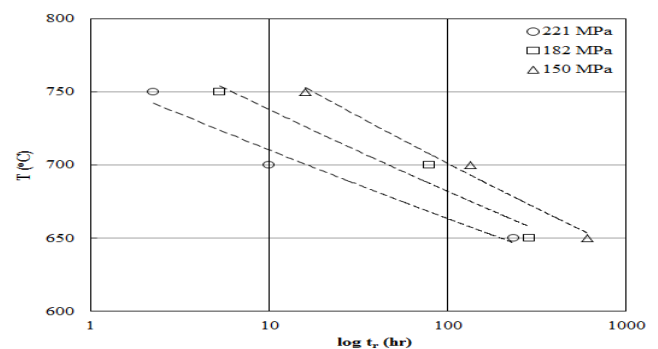


Fig. 6. shows the different parameterization curves obtained in each case.

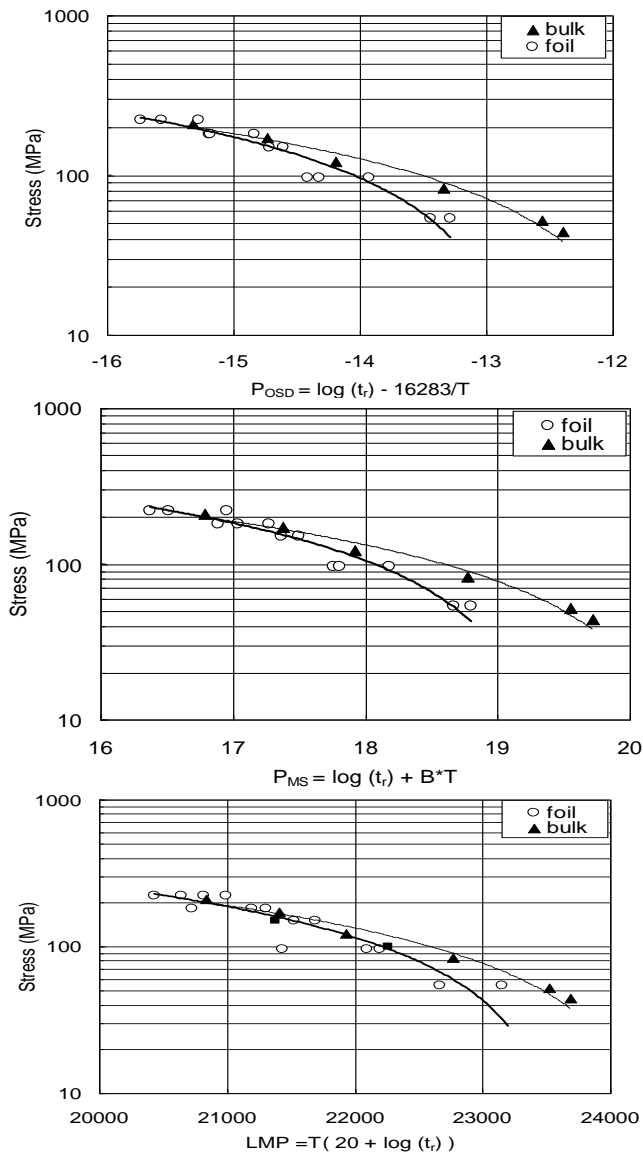


Fig. 7. shows the different parameterization curves obtained in each case. It can be noticed that the results are approximately equivalent, with a slightly better fit for the Manson-Succop and the Manson-Haferd analysis.

V. CONCLUSION

In this study creep life and behaviors of accelerated creep rupture for AISI 347 steel foil, show that:

- 1) The minimum creep rate increases with increasing temperature or stress, causing accelerated rupture at higher temperature or stress.
- 2) In a time 104 s (about 3 hours) the foils specimen deform elastically with some specimen tested under higher stress level deformed with power law creep mechanism, and of order 10⁻⁴ to 10⁻³. At low level of applied stress the strain for the foil reached already the order of 10% with

diffusional flow domination mechanism and at higher stress level Power law mechanism is dominated.

- 3) Iso-stress life prediction methods can be used to extrapolate the results obtained from accelerated creep rupture test. The Manson–Succop method offered the highest degree of fit.
- 4) The mean activation energy for creep was calculated as 676 KJ/molK.
- 5) The higher value in the apparent activation energy indicates that AISI 347 stainless steel exhibits stronger creep resistance than other austenitic stainless steel during rolling at high temperature. This is presumably due to the high content of Nb at 0.7 % in the AISI 347 stainless steel

REFERENCES

- [1] D. Aquaro, and M. Pieve, Compact Heat Exchangers Optimization Developing a Model for the Thermal-Fluid Dynamic Sizing, Int. J. of Heat Technology, vol. 25, pp. 9-18, 2007.
- [2] S.H. Avner, Introduction to Physical Metallurgy, McGraw-Hill International, New York, USA, 1974.
- [3] E. Lara-Curzio, R. Trejo, K.L. More, P.A. Maziasz and B.A. Pint, Screening and Evaluation of Materials for Microturbine Recuperators. Proc. ASME Turbo Expo 2004 Power for Land, Sea, and Air. Vienna, Austria. (2004).
- [4] Y. Minami, H. Kimura and M. Tanimura, Creep Rupture Properties of 18 pct Cr-8pct Ni-Ti-Nb and Type 347H Austenitic Stainless Steels. J. Mater Energy Syst. 7 (1985) 45-55.
- [5] P. J. Maziasz, R. W. Swindeman, Selecting and Developing Advanced Alloys for Creep-Resistance for Microturbine Recuperator Applications, J. Engineering for Gas Turbines and Power Trans of the ASME. 125 (2003) 310-315.
- [6] P.J. Maziasz, B.A. Pint, J.P. Shingledecker, K.L. More, D.E. Evans, and E. Lara-Curzio, Austenitic Stainless Steels and Alloys with Improved High-Temperature Performance for Advanced Microturbine Applications, ASME. 6 (2004) 131-143.
- [7] F.R. Larson, J.A. Miller, Trans. ASME. 74 (1952) 765-771.
- [8] R.L. Orr, O.D. Sherby, and J.E. Dorn, Trans. ASM. 46 (1956) 113-26.
- [9] Stefan Holmström, Rami Pohja, Asta Nurmela, Pekka Moilanen, Pertti Auerkari, Creep and Creep-fatigue Behaviour of 316 Stainless Steel. Procedia Engineering Volume 55, 2013, Pages 160-164
- [10] Husam Al-Warmizyari, Ahmed Naif Alkhazraji, Samir Amin, Creep Strength Degradation for Austenitic Stainless Steel Type 321H Due to Long-Term Service July 2017 Journal of Applied Sciences Research 13(6):26-33
- [11] Avner SH. Introduction to physical metallurgy. 1st ed. New York: McGraw-Hill International, 1974.
- [12] ASTM E139-11 (2011) Standard Method for Conducting Creep, Creep-Rupture, and Stress-Rupture Tests of Metallic Materials
- [13] Deformation-Mechanism Maps, the Plasticity and Creep of Metals and Ceramics, Harold J Frost, and Michael F Ashby Deformation-Mechanism Maps.
- [14] Bueno L O and Sordi V L 2008 Mater. Sci. Eng. A483–484 560 Castilo R, Koul A K and Toscano E H 1987 ASME J. Eng. Gas Turb. Power 109 99
- [15] Orr R, Sherby O D and Dorn J E 1954 Trans. ASME 46 113
- [16] Larson F R and Miller J 1952 Trans. ASME 756
- [17] Koul A K and Castilo R 1988 Metall. Trans. A19 2049
- [18] Marahleh G, Kheder A R I and Hamad H F 2006 Mater. Sci. Eng. A433 305
- [19] LUO,Hai-wen, LI,Hong. FANG, Xu-dong. Constitutive Analysis in Hot Working of a Nb Heavily Alloyed Stainless Steel. J. Iron and Steel Research, International, Volume 14, Issue 5, (2007), Pages 179-182